

Fidelity of Fock-state-encoded qubits subjected to continuous variable Gaussian processes

Brian Julsgaard* and Klaus Mølmer

*Department of Physics and Astronomy, Aarhus University,
Ny Munkegade 120, DK-8000 Aarhus C, Denmark.*

(Dated: March 7, 2018)

When a harmonic oscillator is under the influence of a Gaussian process such as linear damping, parametric gain, and linear coupling to a thermal environment, its coherent states are transformed into states with Gaussian Wigner function. Qubit states can be encoded in the $|0\rangle$ and $|1\rangle$ Fock states of a quantum harmonic oscillator, and it is relevant to know the fidelity of the output qubit state after a Gaussian process on the oscillator. In this paper we present a general expression for the average qubit fidelity in terms of the first and second moments of the output from input coherent states subjected to Gaussian processes.

PACS numbers: 03.67.-a, 03.67.Hk

I. INTRODUCTION

In analogy with the classical bit in computer science, the qubit forms the most basic building block within the field of quantum information [1]. In order to perform quantum computation one must, among other tasks, be able to initialize, manipulate, and read out the information encoded in qubits, and in a scalable implementation it is necessary to store quantum information and transport it from one place or medium to another. Such operations are applied in quantum memories for few-photon light pulses in single atoms [2, 3] and in quantum teleportation between similar qubits [4, 5]. In parallel to qubit-based quantum information science there has also been attention to continuous-variable versions of quantum computation [6], quantum teleportation [7–9], and quantum memories [10–14]. These protocols can be implemented in, e.g., quadrature variables of electromagnetic fields [7], atomic or solid state ensembles of spins [15, 16], or vibration modes of nano-mechanical oscillators [17–21], which are all exact or excellent approximate realizations of the quantum harmonic oscillator.

While the discrete and continuous variable versions of quantum information originally seemed as detached scientific domains, there have been demonstrations of single light quanta, discrete in nature, transferred into the collective spin degrees of freedom of macroscopic atomic ensembles, which are continuous in nature [22–24]. More recently, quantum memories for photonic qubits have been implemented benefiting from the increased collective interaction strength of atomic ensembles compared to single atoms [25–27]. In connection with the use of hybrid physical systems for quantum information processing, multiple proposals exist, making use of the interconnection of mesoscopic qubit degrees of freedom and the continuous variables of ensembles of microscopic systems, nano-mechanical resonators and quantized field modes

[25, 28–35].

The present manuscript addresses an important question in this context: If the transformation properties of continuous variables are known for a particular process in a given physical system, then what can be said about a qubit encoded into the same system and subjected to the same transformation? Specifically, if a harmonic oscillator is subjected to a Gaussian process, characterized by its effect on the first and second moments of the conjugate variables \hat{X} and \hat{P} , we present a general formula for the qubit fidelity, i.e. the probability that the input state of a qubit encoded into the $|0\rangle$ and $|1\rangle$ Fock states of the harmonic oscillator coincide with the output state after the system has been exposed to the process. A Gaussian process can be characterized completely by its action on a small set of coherent states [36], and as pointed out in Ref. [8] this is easier than preparing qubit states for experimental determination of its fidelity. Also, from a theoretical perspective, as exemplified by Ref. [37], the quantum memory fidelity for qubit states can be calculated more easily in a multi-mode set-up by using coherent input states and accounting solely for the first and second moments of the physical variables involved.

The paper is arranged as follows: In Sec. II we show how the observed first and second moments of output states, following from application of coherent input states to the process, yield a convenient parametrization of the Gaussian process. In Sec. III we derive the average fidelity over all qubit states encoded in the $|0\rangle$ and $|1\rangle$ Fock states and subjected to the Gaussian process. In Sec. IV, we present some specific examples, and in Sec. V we conclude the manuscript.

II. PARAMETRIZING THE GAUSSIAN PROCESS

We consider a process, which maps an input quantum state of a single harmonic oscillator to an output state on the same or a different oscillator. For instance this could represent the storage of a radiation-field state into

* brianj@phys.au.dk

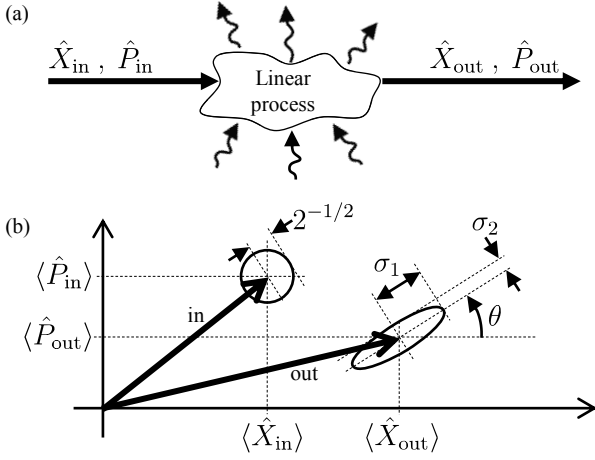


FIG. 1. (a) A single mode of a harmonic oscillator is subjected to a Gaussian process, which maps the input observables \hat{X}_{in} and \hat{P}_{in} into the output variables \hat{X}_{out} and \hat{P}_{out} , of the same or a different quantum system. The wavy arrows represent, e.g., absorption losses or addition of thermal noise associated with the possible coupling to environment degrees of freedom. (b) Schematic view of the transformation of a coherent input state with $\text{Var}(\hat{X}_{\text{in}}) = \text{Var}(\hat{P}_{\text{in}}) = \frac{1}{2}$. The solid arrows indicate the mean values, and the circle and the ellipse show the standard deviation of the continuous quadrature variables in the xp -plane. For the output state, θ denotes the angle between the x -axis and the major axis of the uncertainty ellipse with $\sigma_1 \geq \sigma_2$.

polarization modes of a spin ensemble [10], or it could represent the teleportation of the quadrature amplitudes from one laser beam to another [7]. Figure 1(a) shows schematically how this process transforms the input harmonic oscillator mode $(\hat{X}_{\text{in}}, \hat{P}_{\text{in}})$ into the output mode $(\hat{X}_{\text{out}}, \hat{P}_{\text{out}})$ under the possible influence of the environment. For any input state density matrix $\hat{\rho}_{\text{in}}$ this process is mathematically described by a map, $\hat{\rho}_{\text{out}} = E(\hat{\rho}_{\text{in}})$, and our task is to (i) establish a suitable parametrization of this map, and to (ii) calculate the fidelity when a qubit state is subjected to the process.

The restriction to Gaussian processes relies on two assumptions about the map E . The first one is that it is linear in the sense that our input and output harmonic oscillator modes couple linearly to each other and to all auxiliary reservoir modes. Thus we assume that $(\hat{X}_{\text{in}}, \hat{P}_{\text{in}})$, $(\hat{X}_{\text{out}}, \hat{P}_{\text{out}})$, and the reservoir variables (\hat{x}_j, \hat{p}_j) with $j = 1, \dots, n$, obey the equation:

$$\begin{bmatrix} \hat{X}_{\text{out}} \\ \hat{P}_{\text{out}} \\ \hat{x}_1^{\text{out}} \\ \hat{p}_1^{\text{out}} \\ \vdots \\ \hat{x}_n^{\text{out}} \\ \hat{p}_n^{\text{out}} \end{bmatrix} = \mathbf{A} \begin{bmatrix} \hat{X}_{\text{in}} \\ \hat{P}_{\text{in}} \\ \hat{x}_1^{\text{in}} \\ \hat{p}_1^{\text{in}} \\ \vdots \\ \hat{x}_n^{\text{in}} \\ \hat{p}_n^{\text{in}} \end{bmatrix}, \quad (1)$$

where \mathbf{A} is a $2(n+1) \times 2(n+1)$ matrix. To preserve

canonical commutator relations, \mathbf{A} must be a symplectic matrix [38], which we shall of course assume to hold in the following. The first two rows of this set of equations can be rewritten as:

$$\begin{bmatrix} \hat{X}_{\text{out}} \\ \hat{P}_{\text{out}} \end{bmatrix} = \begin{bmatrix} A_{11} & A_{12} \\ A_{21} & A_{22} \end{bmatrix} \begin{bmatrix} \hat{X}_{\text{in}} \\ \hat{P}_{\text{in}} \end{bmatrix} + \begin{bmatrix} \hat{F}_x \\ \hat{F}_p \end{bmatrix}, \quad (2)$$

where, $\hat{\mathbf{F}} = [\hat{F}_x \hat{F}_p]^T$, are noise operators and represent the combined influence of the reservoir modes.

Our second assumption about E is that all the reservoir modes are described by Gaussian states and are uncorrelated to the input state, $\langle \hat{X}_{\text{in}} \hat{F}_x \rangle = \langle \hat{X}_{\text{in}} \rangle \langle \hat{F}_x \rangle$, etc. This means in particular that the operators $\hat{\mathbf{F}}$ show Gaussian fluctuations, and in order to preserve the commutation relation of the output mode it is required that $[\hat{F}_x, \hat{F}_p] = i(1 - \det(\tilde{\mathbf{A}}))$, where $\tilde{\mathbf{A}}$ is the upper 2×2 block of \mathbf{A} used in Eq. (2). The second moments of the input operators, the output operators, and the noise operators are all given by covariance matrices. For instance, for the output mode the covariance matrix reads $\gamma_{\text{out}} = \langle 2\text{Re}\{\delta\hat{\mathbf{y}}_{\text{out}} \cdot \delta\hat{\mathbf{y}}_{\text{out}}^T\} \rangle$, where the vector $\hat{\mathbf{y}}_{\text{out}} = [\hat{X}_{\text{out}} \hat{P}_{\text{out}}]^T$ and where $\hat{\mathbf{y}}_{\text{out}} = \langle \hat{\mathbf{y}}_{\text{out}} \rangle + \delta\hat{\mathbf{y}}_{\text{out}}$ defines the fluctuations of operators around their mean values. The output mode covariance matrix thus reads:

$$\gamma_{\text{out}} = 2 \begin{bmatrix} \text{Var}(\hat{X}_{\text{out}}) & \text{Cov}(\hat{X}_{\text{out}}, \hat{P}_{\text{out}}) \\ \text{Cov}(\hat{X}_{\text{out}}, \hat{P}_{\text{out}}) & \text{Var}(\hat{P}_{\text{out}}) \end{bmatrix}, \quad (3)$$

where $\text{Cov}(\hat{X}_{\text{out}}, \hat{P}_{\text{out}}) = \frac{1}{2} \langle \delta\hat{X}_{\text{out}} \delta\hat{P}_{\text{out}} + \delta\hat{P}_{\text{out}} \delta\hat{X}_{\text{out}} \rangle$. Similar covariance matrices γ_{in} and γ_F are defined for the input and the noise parts, respectively. The second moments of the operators, i.e., the covariance matrices, fulfill:

$$\gamma_{\text{out}} = \tilde{\mathbf{A}} \gamma_{\text{in}} \tilde{\mathbf{A}}^T + \gamma_F. \quad (4)$$

It was shown recently that coherent states suffice as input states to fully characterize a process on harmonic oscillator modes [39], and in the case of a Gaussian process with the linear transformation (1) of the canonical variables, a small discrete set of coherent states is enough to yield the complete information about the process [36]. Gaussian states are described completely by their first and second moments, and the matrix $\tilde{\mathbf{A}}$, the two mean values $\langle \hat{F}_x \rangle$ and $\langle \hat{F}_p \rangle$, and the three real parameters of γ_F are sufficient to describe the entire Gaussian process. We shall now show how the process may equivalently be characterized by the quantities indicated in Fig. 1(a), which are experimentally available when applying coherent input states to the process.

For the vacuum input state $\langle \hat{X}_{\text{out}} \rangle = \langle \hat{F}_x \rangle$ and $\langle \hat{P}_{\text{out}} \rangle = \langle \hat{F}_p \rangle$ map out the mean values of the noise operators of the environment, and then two other coherent input states with non-zero mean values suffice to map out the entries of the matrix $\tilde{\mathbf{A}}$, since $\langle \hat{\mathbf{y}}_{\text{out}} \rangle = \tilde{\mathbf{A}} \langle \hat{\mathbf{y}}_{\text{in}} \rangle + \langle \hat{\mathbf{F}} \rangle$. In turn, since γ_{in} is the identity matrix for any coherent state, the second moments of the output mode operators establish the relations, $\text{Var}(\hat{F}_x) = \text{Var}(\hat{X}_{\text{out}}) -$

$\frac{1}{2}(A_{11}^2 + A_{12}^2)$, $\text{Var}(\hat{F}_p) = \text{Var}(\hat{P}_{\text{out}}) - \frac{1}{2}(A_{21}^2 + A_{22}^2)$, and $\text{Cov}(\hat{F}_x, \hat{F}_p) = \text{Cov}(\hat{X}_{\text{out}}, \hat{P}_{\text{out}}) - \frac{1}{2}(A_{11}A_{21} + A_{12}A_{22})$. In the following, we assume without loss of generality that $\langle \hat{F}_x \rangle = \langle \hat{F}_p \rangle = 0$, since any known non-zero mean value added to the output mode can be readily identified by experiment and subtracted by a simple displacement, which will not degrade our knowledge of the quantum state. It is convenient to use the parametrization for the second moments of the output mode shown in Fig. 1(b), i.e., the variances, σ_1^2 and σ_2^2 , along the main axes of the “noise ellipse” and the angle θ between the x -axis and the major axis of the noise ellipse. These variables relate to the parameters $\sigma_x^2 = \text{Var}(\hat{X}_{\text{out}})$, $\sigma_p^2 = \text{Var}(\hat{P}_{\text{out}})$, and $C_{x,p} = \text{Cov}(\hat{X}_{\text{out}}, \hat{P}_{\text{out}})$ of γ_{out} by:

$$\begin{aligned} \sigma_1^2 &= \bar{\sigma}^2 + \delta\sigma^2, \quad \sigma_2^2 = \bar{\sigma}^2 - \delta\sigma^2, \quad \tan(2\theta) = \frac{2C_{x,p}}{\sigma_x^2 - \sigma_p^2}, \\ \text{with } \bar{\sigma}^2 &= \frac{\sigma_x^2 + \sigma_p^2}{2}, \quad \delta\sigma^2 = \sqrt{\frac{1}{4}(\sigma_x^2 - \sigma_p^2)^2 + C_{x,p}^2}. \end{aligned} \quad (5)$$

If $C_{x,p}$ is positive (negative), $0 < \theta < \frac{\pi}{2}$ ($-\frac{\pi}{2} < \theta < 0$), while if $\sigma_x^2 = \sigma_p^2$ and $C_{x,p} \neq 0$ we assume $\theta = \frac{\pi}{4}\text{sign}(C_{x,p})$.

For a coherent input state, $\hat{\rho}_{\text{in}} = |\alpha\rangle\langle\alpha|$, the output state $\hat{\rho}_{\text{out}}$ can always be described by a displaced, squeezed, thermal state, offering enough variables to parametrize the Gaussian state, illustrated in Fig. 1(b). We shall now provide a convenient expression of this output state as a function of the coherent state amplitude, α , and the parameters, A_{11} , A_{12} , A_{21} , A_{22} , σ_1^2 , σ_2^2 , and θ , discussed above. To this end we define first the thermal state:

$$\hat{\rho}_0 = \frac{1}{\pi\bar{n}_0} \int d^2\gamma e^{-|\gamma|^2/\bar{n}_0} |\gamma\rangle\langle\gamma|, \quad (6)$$

where the integral is carried out over all coherent states $|\gamma\rangle$. Applying the squeezing operator $\hat{S}(r) = e^{\frac{r}{2}(\hat{a}^2 - \hat{a}^{\dagger 2})}$, where r is a real parameter, to the thermal state we obtain the squeezed thermal state: $\hat{\rho}_{\text{STS}} = \hat{S}(r)\hat{\rho}_0\hat{S}^\dagger(r)$ with well-known properties [40]. With the standard definitions $\hat{X} = \frac{\hat{a} + \hat{a}^\dagger}{\sqrt{2}}$ and $\hat{P} = \frac{-i(\hat{a} - \hat{a}^\dagger)}{\sqrt{2}}$ this state has $\text{Var}(\hat{X}) = (\bar{n}_0 + \frac{1}{2})e^{-2r}$ and $\text{Var}(\hat{P}) = (\bar{n}_0 + \frac{1}{2})e^{2r}$. By choosing appropriately the values of \bar{n}_0 and r ,

$$\sigma_1^2 = (\bar{n}_0 + \frac{1}{2})e^{-2r}, \quad \sigma_2^2 = (\bar{n}_0 + \frac{1}{2})e^{2r}. \quad (7)$$

and applying, finally, the rotation operator $\hat{R}(\theta) = e^{i\theta\hat{a}^\dagger\hat{a}}$ we obtain a rotated squeezed thermal state,

$$\hat{\rho}_r = \hat{R}(\theta)\hat{\rho}_{\text{STS}}\hat{R}^\dagger(\theta), \quad (8)$$

with precisely the noise properties indicated by the output ellipse shown in Fig. 1(b).

The correct dependence of the output state mean values on the amplitude of the input coherent state is reproduced by applying the displacement operator $\hat{D}(\bar{\alpha}) =$

$e^{\bar{\alpha}\hat{a}^\dagger - \bar{\alpha}^*\hat{a}}$ to $\hat{\rho}_r$ such that a coherent input state is mapped to the output state,

$$E(|\alpha\rangle\langle\alpha|) = \hat{\rho}_\alpha, \quad (9)$$

with

$$\begin{aligned} \hat{\rho}_\alpha &= \hat{D}(\bar{\alpha})\hat{R}(\theta)\hat{S}(r)\hat{\rho}_0\hat{S}^\dagger(r)\hat{R}^\dagger(\theta)\hat{D}^\dagger(\bar{\alpha}), \\ \begin{bmatrix} \bar{\alpha}_R \\ \bar{\alpha}_I \end{bmatrix} &= \begin{bmatrix} A_{11} & A_{12} \\ A_{21} & A_{22} \end{bmatrix} \begin{bmatrix} \alpha_R \\ \alpha_I \end{bmatrix}, \end{aligned} \quad (10)$$

where “R” and “I” refer to the real and imaginary parts, respectively, of input mean amplitude α and output mean amplitude $\bar{\alpha}$. It is convenient to introduce the equivalent relations between α and $\bar{\alpha}$ in complex notation:

$$\begin{aligned} \bar{\alpha} &= C\alpha + D\alpha^*, \\ C &= \frac{1}{2}(A_{11} - iA_{12} + iA_{21} + A_{22}), \\ D &= \frac{1}{2}(A_{11} + iA_{12} + iA_{21} - A_{22}). \end{aligned} \quad (11)$$

We note that rather than presenting a map on the input coherent state, Eq. (10) formally provides the output state as an α -dependent transformation of a definite input state: $|\alpha\rangle\langle\alpha| \rightarrow E(|\alpha\rangle\langle\alpha|) \equiv \hat{D}(\bar{\alpha})\hat{\rho}_r\hat{D}^\dagger(\bar{\alpha})$. This form is, however, perfectly useful to characterize the process and it is a good starting point for our analysis of the qubit fidelity in the next section.

III. DERIVATION OF THE QUBIT FIDELITY FORMULA

From the coherent-state expansion on the Fock-state basis,

$$|\alpha\rangle = e^{-\frac{|\alpha|^2}{2}} \sum_{n=0}^{\infty} \frac{\alpha^n}{\sqrt{n!}} |n\rangle, \quad (12)$$

we see that the Fock basis states can be formally obtained from expressions involving coherent states by $|n\rangle = \frac{1}{\sqrt{n!}} \frac{\partial^n}{\partial \alpha^n} [e^{\frac{|\alpha|^2}{2}} |\alpha\rangle]_{\alpha=0}$. In turn, due to the linearity of the map E , its action on a general Fock state outer product can be retrieved as:

$$E(|n\rangle\langle m|) = \frac{1}{\sqrt{n!m!}} \frac{\partial^n}{\partial \alpha^n} \frac{\partial^m}{\partial \alpha^{*m}} [e^{|\alpha|^2} E(|\alpha\rangle\langle\alpha|)]_{\alpha=0}. \quad (13)$$

Any qubit state expanded on the Fock states $|n=0\rangle$ and $|n=1\rangle$ can thus be mapped if we know the quantities $E(|n=0\rangle\langle n=0|) = E(|\alpha=0\rangle\langle\alpha=0|)$, $E(|1\rangle\langle 0|) = \frac{\partial}{\partial \alpha} E(|\alpha\rangle\langle\alpha|)_{\alpha=0}$, $E(|0\rangle\langle 1|) = \frac{\partial}{\partial \alpha^*} E(|\alpha\rangle\langle\alpha|)_{\alpha=0}$, and $E(|1\rangle\langle 1|) = (1 + \frac{\partial^2}{\partial \alpha \partial \alpha^*}) E(|\alpha\rangle\langle\alpha|)_{\alpha=0}$.

The derivatives can be expressed in terms of $\bar{\alpha}$ using

Eq. (11):

$$\begin{aligned}\frac{\partial}{\partial \alpha} &= C \frac{\partial}{\partial \bar{\alpha}} + D^* \frac{\partial}{\partial \bar{\alpha}^*}, \\ \frac{\partial}{\partial \alpha^*} &= D \frac{\partial}{\partial \bar{\alpha}} + C^* \frac{\partial}{\partial \bar{\alpha}^*}, \\ \frac{\partial^2}{\partial \alpha \partial \alpha^*} &= CD \frac{\partial^2}{\partial \bar{\alpha}^2} + (|C|^2 + |D|^2) \frac{\partial^2}{\partial \bar{\alpha} \partial \bar{\alpha}^*} + (CD)^* \frac{\partial^2}{\partial \bar{\alpha}^{*2}}.\end{aligned}\quad (14)$$

Only the displacement operators in Eq. (10) depend on the coherent state amplitudes, and their derivatives are given by $\frac{\partial \hat{D}(\bar{\alpha})}{\partial \bar{\alpha}} = \left(\hat{a}^\dagger - \frac{\bar{\alpha}^*}{2}\right) \hat{D}(\bar{\alpha})$, $\frac{\partial \hat{D}(\bar{\alpha})}{\partial \bar{\alpha}^*} = -\left(\hat{a} - \frac{\bar{\alpha}}{2}\right) \hat{D}(\bar{\alpha})$, and their hermitian conjugates. The first and second derivatives of $E(|\alpha\rangle\langle\alpha|)$ with respect to $\bar{\alpha}$ and $\bar{\alpha}^*$ are thus given by

$$\begin{aligned}\frac{\partial E}{\partial \bar{\alpha}} &= \hat{a}^\dagger \hat{\rho}_r - \hat{\rho}_r \hat{a}^\dagger, \\ \frac{\partial E}{\partial \bar{\alpha}^*} &= -\hat{a} \hat{\rho}_r + \hat{\rho}_r \hat{a}, \\ \frac{\partial^2 E}{\partial \bar{\alpha}^2} &= \hat{a}^{\dagger 2} \hat{\rho}_r - 2\hat{a}^\dagger \hat{\rho}_r \hat{a}^\dagger + \hat{\rho}_r \hat{a}^{\dagger 2}, \\ \frac{\partial^2 E}{\partial \bar{\alpha}^{*2}} &= \hat{a}^2 \hat{\rho}_r - 2\hat{a} \hat{\rho}_r \hat{a} + \hat{\rho}_r \hat{a}^2, \\ \frac{\partial^2 E}{\partial \bar{\alpha} \partial \bar{\alpha}^*} &= -\hat{a}^\dagger \hat{a} \hat{\rho}_r + \hat{a}^\dagger \hat{\rho}_r \hat{a} + \hat{a} \hat{\rho}_r \hat{a}^\dagger - \hat{\rho}_r \hat{a} \hat{a}^\dagger,\end{aligned}\quad (15)$$

where $\hat{\rho}_r$ is given in Eq. (8), and the right hand sides are formally independent of α (the derivatives are evaluated at $\alpha = 0$).

The fidelity is defined as the overlap of the state subject to the transformation E with the original qubit state and thus requires matrix elements of the left-hand side of Eq. (13) between the Fock states $|0\rangle$ and $|1\rangle$. In turn, using Eqs. (13)-(15) this is equivalent to calculating matrix element of the right-hand side of Eq. (15) between the Fock states $|0\rangle$ and $|1\rangle$. Now, due to the raising and lowering operators in this equation (up to quadratic order) we end up with matrix elements on the form $\langle n' | \hat{\rho}_r | m' \rangle = e^{i\theta(n'-m')} \langle n' | \hat{\rho}_{\text{STS}} | m' \rangle$, where the integers n' and m' may take values from 0 to 3. For instance, we have $\langle 1 | E(|1\rangle\langle 0|) | 0 \rangle = C \langle 1 | \hat{a}^\dagger \hat{\rho}_r - \hat{\rho}_r \hat{a}^\dagger | 0 \rangle + D^* \langle 1 | -\hat{a} \hat{\rho}_r + \hat{\rho}_r \hat{a} | 0 \rangle = C[\langle 0 | \hat{\rho}_{\text{STS}} | 0 \rangle - \langle 1 | \hat{\rho}_{\text{STS}} | 1 \rangle] - \sqrt{2} D^* e^{2i\theta} \langle 2 | \hat{\rho}_{\text{STS}} | 0 \rangle$, and the first term in this expression can be calculated directly as

$$\begin{aligned}\langle 0 | \hat{\rho}_{\text{STS}} | 0 \rangle &= \frac{1}{\pi \bar{n}_0} \int d^2 \gamma e^{-|\gamma|^2 / \bar{n}_0} |\langle 0 | \hat{S}(r) | \gamma \rangle|^2 \\ &= \frac{1}{\pi \bar{n}_0 \cosh(r)} \int d^2 \gamma e^{-\frac{1+\bar{n}_0}{\bar{n}_0} |\gamma|^2 + \frac{\gamma^2 + \gamma^{*2}}{2} \tanh(r)} \\ &= \frac{1}{\sqrt{[(\frac{1}{2} + \bar{n}_0) e^{-2r} + \frac{1}{2}] [(\frac{1}{2} + \bar{n}_0) e^{2r} + \frac{1}{2}]}} \\ &= \frac{1}{[(\sigma_1^2 + \frac{1}{2})(\sigma_2^2 + \frac{1}{2})]^{1/2}}.\end{aligned}\quad (16)$$

The first equality, in which $\langle n = 0 |$ refers to the Fock basis and $|\gamma\rangle$ to the coherent-state basis, follows from the expansion (6) of the thermal state on coherent states, the second line exploits the Fock-state expansion of squeezed coherent states [41]:

$$\begin{aligned}\langle n | \hat{S}(r) | \gamma \rangle &= \frac{e^{-\frac{|\gamma|^2}{2} + \frac{\gamma^2}{2} \tanh(r)}}{\sqrt{n! \cosh(r)}} \left(\frac{1}{2} \tanh(r) \right)^{\frac{n}{2}} \\ &\quad \times H_n \left(\gamma / \sqrt{\sinh(2r)} \right),\end{aligned}\quad (17)$$

where H_n is a Hermite polynomial, the third line carries out the γ -integration, and the last step applies the relations in Eq. (7). Similar calculations are readily performed for the remaining relevant matrix elements and yield:

$$\begin{aligned}\langle 1 | \hat{\rho}_{\text{STS}} | 1 \rangle &= \frac{\sigma_1^2 \sigma_2^2 - \frac{1}{4}}{[(\sigma_1^2 + \frac{1}{2})(\sigma_2^2 + \frac{1}{2})]^{3/2}}, \\ \langle 0 | \hat{\rho}_{\text{STS}} | 2 \rangle &= \frac{\sigma_1^2 - \sigma_2^2}{2\sqrt{2}[(\sigma_1^2 + \frac{1}{2})(\sigma_2^2 + \frac{1}{2})]^{3/2}}, \\ \langle 2 | \hat{\rho}_{\text{STS}} | 2 \rangle &= \frac{(\sigma_1^2 \sigma_2^2 - \frac{1}{4})^2 + \frac{1}{8}(\sigma_1^2 - \sigma_2^2)^2}{[(\sigma_1^2 + \frac{1}{2})(\sigma_2^2 + \frac{1}{2})]^{5/2}}, \\ \langle 1 | \hat{\rho}_{\text{STS}} | 3 \rangle &= \frac{\sqrt{6}(\sigma_1^2 \sigma_2^2 - \frac{1}{4})(\sigma_1^2 - \sigma_2^2)}{4[(\sigma_1^2 + \frac{1}{2})(\sigma_2^2 + \frac{1}{2})]^{5/2}}.\end{aligned}\quad (18)$$

By integrating the fidelity for any input qubit state, $|\psi(\Omega)\rangle = \cos \frac{\theta}{2} |0\rangle + e^{i\phi} \sin \frac{\theta}{2} |1\rangle$ with $0 \leq \theta \leq \pi$ and $0 \leq \phi \leq 2\pi$, we determine the average qubit fidelity F_q :

$$\begin{aligned}F_q &= \frac{1}{4\pi} \int d\Omega \langle \psi(\Omega) | E(|\psi(\Omega)\rangle\langle\psi(\Omega)|) | \psi(\Omega) \rangle \\ &= \frac{1}{3} [\langle 0 | E(|0\rangle\langle 0|) | 0 \rangle + \langle 1 | E(|1\rangle\langle 1|) | 1 \rangle] \\ &\quad + \frac{1}{6} [\langle 0 | E(|0\rangle\langle 1|) | 1 \rangle + \langle 1 | E(|1\rangle\langle 0|) | 0 \rangle] \\ &\quad + \frac{1}{6} [\langle 1 | E(|0\rangle\langle 0|) | 1 \rangle + \langle 0 | E(|1\rangle\langle 1|) | 0 \rangle],\end{aligned}\quad (19)$$

where $|0\rangle$ and $|1\rangle$ refer to Fock states. With the expression derived above, we thus reach the final, explicit expression for the average qubit fidelity in terms of the mapping parameters of the Gaussian process:

$$F_q = \frac{1}{6\sqrt{(\sigma_1^2 + \frac{1}{2})(\sigma_2^2 + \frac{1}{2})}} \left\{ 3 + \frac{3(\sigma_1^2\sigma_2^2 - \frac{1}{4})}{(\sigma_1^2 + \frac{1}{2})(\sigma_2^2 + \frac{1}{2})} + \frac{\text{Re}\{C + \tilde{D}^*\}}{\sigma_1^2 + \frac{1}{2}} + \frac{\text{Re}\{C - \tilde{D}^*\}}{\sigma_2^2 + \frac{1}{2}} \right. \\ \left. - \frac{|C + \tilde{D}^*|^2(\sigma_1^2 - 1)}{(\sigma_1^2 + \frac{1}{2})^2} - \frac{|C - \tilde{D}^*|^2(\sigma_2^2 - 1)}{(\sigma_2^2 + \frac{1}{2})^2} - \frac{|C + \tilde{D}^*|^2(\sigma_2^2 - \frac{1}{2}) + |C - \tilde{D}^*|^2(\sigma_1^2 - \frac{1}{2})}{2(\sigma_1^2 + \frac{1}{2})(\sigma_2^2 + \frac{1}{2})} \right\}, \quad (20)$$

where $\tilde{D} = De^{-2i\theta}$. This is the main results of the article, and in the next section we shall consider the fidelity formula in various specific cases, corresponding to the experimental storage and transfer schemes mentioned in the Introduction.

Let us briefly discuss the different effects contributing to a reduction of the fidelity. First, we observe that Eq. (20) decreases when $\sigma_{1,2}$ become large. This is natural, as the qubit occupies only the lowest two Fock states, while the output state is distributed toward higher number states $n \propto \sigma_1^2, \sigma_2^2$, and hence a corresponding smaller fraction of the population remains in the qubit space. Even with $\sigma_{1,2}$ close to the minimum allowed by the Heisenberg uncertainty relation, the values of C, D and θ can lead to large variations in the qubit fidelity. This is associated with the possibility for the map to yield an (undesired) unitary operation on the qubit, e.g., in the form of a rotation of the Bloch vector around the z -axis, caused by a rotation of the continuous quadrature variables in the (\hat{X}, \hat{P}) phase space. Thus, the unitary mapping $\hat{X}_1 \rightarrow -\hat{X}_1$ and $\hat{P}_1 \rightarrow -\hat{P}_1$, represented by $A_{11} = A_{22} = -1$, $A_{12} = A_{21} = 0$, and $\sigma_1^2 = \sigma_2^2 = \frac{1}{2}$, yields, according to Eq. (20), an average qubit fidelity $F_q = \frac{1}{3}$. The mapping, however, is perfect, if we only redefine the basis states by a simple phase change of $-\pi$ after the process, and it makes sense to allow incorporation of such a trivial transformation in the definition of the average qubit fidelity. The effect on Eq. (20) of a phase rotation by θ' corresponds to setting $C \rightarrow Ce^{i\theta'}$ and $\tilde{D}^* \rightarrow \tilde{D}^*e^{i\theta'}$, which affects only the two terms linear in C and \tilde{D}^* in Eq. (20). The angles θ' yielding the extremal values of F_q are thus given by:

$$e^{2i\theta'} = \frac{(C^* + \tilde{D})(\sigma_2^2 + \frac{1}{2}) + (C^* - \tilde{D})(\sigma_1^2 + \frac{1}{2})}{(C + \tilde{D}^*)(\sigma_2^2 + \frac{1}{2}) + (C - \tilde{D}^*)(\sigma_1^2 + \frac{1}{2})}. \quad (21)$$

For the simple map with the π rotation, qubit fidelity extrema are found at $\theta' = n\pi$, where n is an integer, and for odd n the rotation is counter-acted and a unit fidelity is recovered.

IV. EXAMPLES

A. Symmetric gain and variance

Consider the specific case where both \hat{X} and \hat{P} are multiplied by the same gain coefficient g in the transformation process such that $A_{11} = A_{22} = g$ and $A_{12} =$

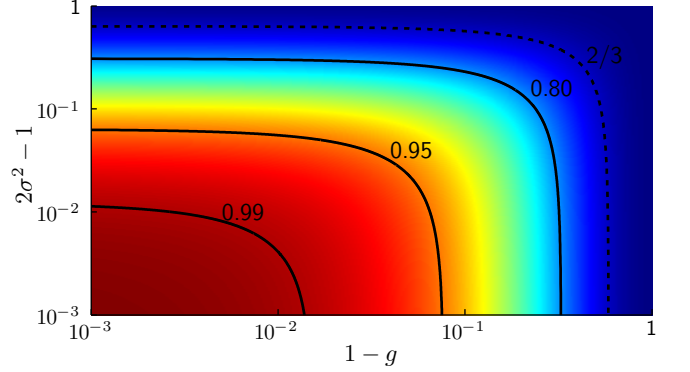


FIG. 2. (Color online) A contour plot of the qubit fidelity for symmetric gain and variances according to Eq. (22) as a function of the gain imperfection, $1 - g$, and the excess variance relative to the vacuum noise limit, $2\sigma^2 - 1$. A few values of F_q are marked on the graph with the dashed curve enclosing the non-classical limit $F_q > \frac{2}{3}$.

$A_{21} = 0$. Assume also the added noise to be symmetric, $\sigma_1^2 = \sigma_2^2 = \sigma^2$. Then the fidelity becomes

$$F_q = \frac{6\sigma^4 + 3\sigma^2 + g(2\sigma^2 + 1) - g^2(3\sigma^2 - \frac{5}{2})}{6(\sigma^2 + \frac{1}{2})^3}, \quad (22)$$

which is identical to the result found in [8]. The value of F_q as a function of g and σ^2 is shown in Fig. 2.

By a projective qubit measurement, one obtains an outcome that may be stored by classical means, and the corresponding eigenstate may be reinstalled in the physical output system at any later time. This classical procedure provides a qubit state with an average overlap with the unknown initial state of $2/3$ [43]. The dashed curve with $F_q = 2/3$ in Fig. 2 represents the benchmark value where a quantum storage or transfer operation outperforms the much simpler classical strategy.

B. An oscillator coupled to a heat bath

Consider a harmonic oscillator, e.g. a cavity field with resonance frequency ω_0 , coupled by an energy-decay rate γ to an external heat bath at temperature T . The characteristic number of excitations in the heat bath is $\bar{N} = [\exp(\frac{\hbar\omega_0}{k_B T}) - 1]^{-1}$, and the quantum Langevin equations for the oscillator mode \hat{a} can be written [42]:

$$\frac{\partial \hat{a}}{\partial t} = -i\omega_0 \hat{a} - \frac{\gamma}{2} \hat{a} - \sqrt{\gamma} \hat{b}_{\text{in}}, \quad (23)$$

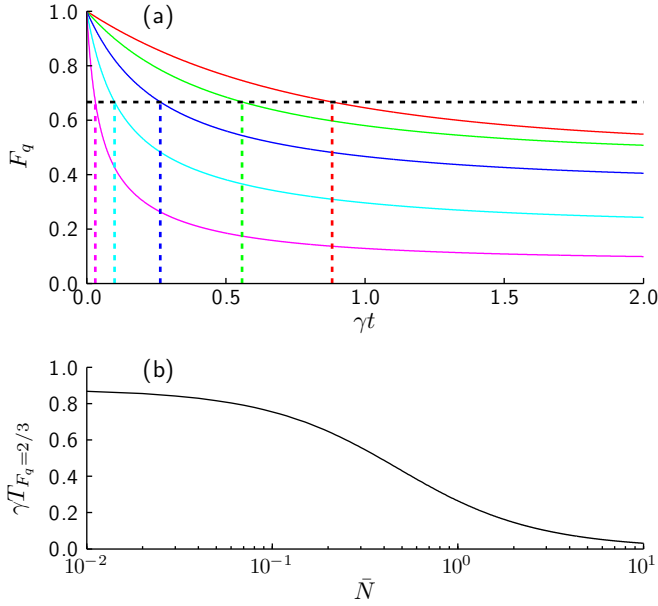


FIG. 3. (Color online) (a) The decay of qubit fidelity when the harmonic oscillator hosting the qubit is coupled to a heat bath by a decay rate γ . Each curve corresponds to a specific bath temperature with \bar{N} denoting the mean excitation level of the oscillator in equilibrium. From above: $\bar{N} = 0$ (red), $\bar{N} = 0.3$ (green), $\bar{N} = 1$ (blue), $\bar{N} = 3$ (cyan), and $\bar{N} = 10$ (magenta). The horizontal dashed line denotes the non-classical limit $F_q > \frac{2}{3}$ and the vertical dashed lines mark the time $T_{F_q=2/3}$ at which this limit is reached. This characteristic time is also shown in (b) on the vertical axis (in units of γ^{-1}) as a function of the equilibrium excitation level \bar{N} .

where \hat{b}_{in} is the input thermal field, which in the broadband approximation satisfies $\langle \hat{b}_{\text{in}}(t)\hat{b}_{\text{in}}^\dagger(t') \rangle = (\bar{N}+1)\delta(t-t')$ and $\langle \hat{b}_{\text{in}}^\dagger(t)\hat{b}_{\text{in}}(t') \rangle = \bar{N}\delta(t-t')$. Eq. (2) yields the solution of Eq. (23) with $g \equiv A_{11} = A_{22} = e^{-\frac{\gamma t}{2}}$ and $A_{12} = A_{21} = 0$. From the properties of \hat{b}_{in} we deduce that $\text{Var}(\hat{F}_x) = \text{Var}(\hat{F}_p) = (\bar{N} + \frac{1}{2})(1 - e^{-\gamma t})$ and $\text{Cov}(\hat{F}_x, \hat{F}_p) = 0$, and hence for a coherent-state input the variances of the output state is $\sigma^2 \equiv \sigma_1^2 = \sigma_2^2 = \frac{1}{2} + \bar{N}(1 - e^{-\gamma t})$. The qubit fidelity now follows from inserting the parameters g and σ^2 into Eq. (22), and the resulting fidelity is shown in Fig. 3.

We observe that the decay of fidelity occurs faster when the heat bath temperature is increased. In Fig. 3(a) the initial linear decrease in F_q follows the approximate formula: $F_q \approx 1 - \frac{(2+5\bar{N})\gamma t}{3}$. In the asymptotic limit $t \rightarrow \infty$ the fidelity converges, $F_q \rightarrow \frac{\bar{N}+\frac{1}{2}}{(\bar{N}+1)^2}$, i.e. for $\bar{N} = 0$ the qubit decays to the ground state $|0\rangle$ which has a 50 % chance of reproducing the random input qubit, and for large \bar{N} the oscillator is most likely excited away from the qubit space spanned by $|0\rangle$ and $|1\rangle$ leading to a vanishing fidelity.

The horizontal dashed line with $F_q = 2/3$ in Fig. 3(a) represents the benchmark value of quantum storage,

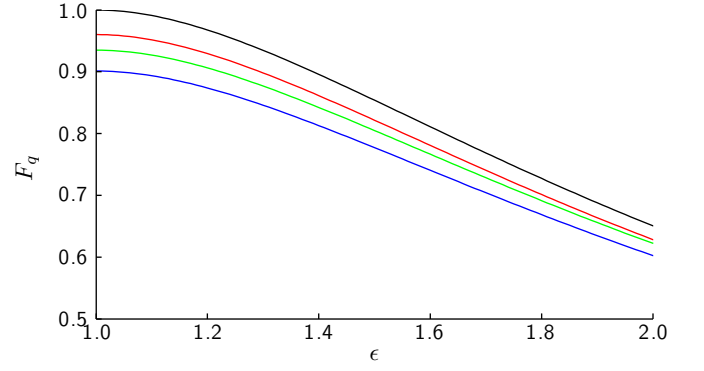


FIG. 4. (Color online) The qubit fidelity from Eq. (25) as a function of ϵ , which is conveniently used to parametrize the asymmetry in gain and variance by $g_x = g_0\epsilon$, $g_p = g_0/\epsilon$, $\sigma_x^2 = \sigma_0^2\epsilon^2$, and $\sigma_p^2 = \sigma_0^2/\epsilon^2$. From the top, $g_0 = 1$ and $\sigma_0^2 = \frac{1}{2}$ (black), $g_0 = 1$ and $\sigma_0^2 = \frac{1.05}{2}$ (red), $g_0 = 0.9$ and $\sigma_0^2 = \frac{1}{2}$ (green), and $g_0 = 0.9$ and $\sigma_0^2 = \frac{1.05}{2}$ (blue).

which occurs at the \bar{N} -dependent times marked by the vertical dashed lines. In Fig. 3(b) these times are shown more generally as a function of \bar{N} . The $\bar{N} \rightarrow 0$ limit yields $\gamma T_{F_q=2/3} \rightarrow -\ln(\sqrt{2}-1) \approx 0.88$, i.e. for an exponentially decreasing coherence, the process supercedes the classical benchmark for times less than 88 % of the coherence time.

C. Asymmetric gain and variance along the same major axes

In most practical cases with asymmetric gain and variance, the asymmetries materialize along the same axes in (\hat{X}, \hat{P}) -space. One example is the degenerate parametric amplifier [44], for which the transformations are $\langle \hat{X}_{\text{out}} \rangle = G\langle \hat{X}_{\text{in}} \rangle$, $\langle \hat{P}_{\text{out}} \rangle = G^{-1}\langle \hat{P}_{\text{in}} \rangle$, $\sigma_x^2 = \frac{G^2}{2}$, $\sigma_p^2 = \frac{1}{2G^2}$, and $C_{x,p} = 0$, i.e. the coordinate system is chosen, without loss of generality, such that the mean value transformation $\hat{\mathbf{A}}$ is diagonal and at the same time it turns out that $\theta = 0$, i.e. the (\hat{X}, \hat{P}) -axes form also the major axes for the covariance matrix γ_{out} . Another example can be found in spin-ensemble based quantum memories, which encode quantum information into the transverse components $\hat{X} \equiv \hat{S}_x/\sqrt{|S_z|}$ and $\hat{P} \equiv -\hat{S}_y/\sqrt{|S_z|}$ of a macroscopic spin polarized along the negative z -direction. For an inhomogeneous distribution of spin frequencies the stored information is “diffused” into the spin ensemble and recalled as a spin echo using a set of π pulses for inverting the ensemble population. These π pulses employ a spin rotation around a certain axis and thereby break the symmetry of the (\hat{X}, \hat{P}) -space, and especially for non-ideal π pulses the transformations (2) and (4) become asymmetric (in some cases even squeezed) [45]. In this case also, $\hat{\mathbf{A}}$ and γ turn out diagonal in a common coordinate system, and the two above examples thus

motivate a closer look on the particular transformation:

$$\tilde{\mathbf{A}} = \begin{bmatrix} g_x & 0 \\ 0 & g_p \end{bmatrix}, \quad \gamma_{\text{out}} = \begin{bmatrix} 2\sigma_x^2 & 0 \\ 0 & 2\sigma_p^2 \end{bmatrix}. \quad (24)$$

As long as the Heisenberg uncertainty relation, $\sigma_x^2 \sigma_p^2 \geq \frac{1}{4}$, is satisfied we allow σ_x^2 and σ_p^2 to take any value meeting the constraints $2\sigma_1^2 \geq g_x^2$ and $2\sigma_2^2 \geq g_p^2$ imposed by Eq. (4) and the positivity of $(\gamma_F)_{11}$ and $(\gamma_F)_{22}$. We may think of this transformations as a noisy parametric amplifier (the version discussed above is a minimum-uncertainty case). When the properties of (24) are inserted into the general formula (20) we find:

$$F_q = \frac{1}{6\sqrt{(\sigma_x^2 + \frac{1}{2})(\sigma_p^2 + \frac{1}{2})}} \left\{ 3 + \frac{3(\sigma_x^2 \sigma_p^2 - \frac{1}{4})}{(\sigma_x^2 + \frac{1}{2})(\sigma_p^2 + \frac{1}{2})} \right. \\ \left. + \frac{g_x}{\sigma_x^2 + \frac{1}{2}} + \frac{g_p}{\sigma_p^2 + \frac{1}{2}} - \frac{g_x^2(\sigma_x^2 - 1)}{(\sigma_x^2 + \frac{1}{2})^2} - \frac{g_p^2(\sigma_p^2 - 1)}{(\sigma_p^2 + \frac{1}{2})^2} \right. \\ \left. - \frac{g_x^2(\sigma_p^2 - \frac{1}{2}) + g_p^2(\sigma_x^2 - \frac{1}{2})}{2(\sigma_x^2 + \frac{1}{2})(\sigma_p^2 + \frac{1}{2})} \right\}. \quad (25)$$

In order to illustrate how the asymmetry affects the qubit fidelity, we show in Fig. 4 a number of curves, where for each curve the products $g_x g_p \equiv g_0^2$ and $\sigma_x^2 \sigma_p^2 \equiv \sigma_0^4$ remain constant but the degree of asymmetry is changed along the horizontal axis, see the figure caption for explanation. We note that the upper curve corresponds to the special case of a noiseless parametric amplifier for which $F_q = \frac{\sqrt{2}}{3} \frac{\cosh(2r) + 2 \cosh(r) + 3}{[1 + \cosh(2r)]^{3/2}}$, where we parametrized the gain as $G = \epsilon = e^r$. This expression for F_q stays above the classical benchmark $\frac{2}{3}$ for $\epsilon \lesssim 1.96$.

V. SUMMARY

In this paper we have presented calculations yielding the average fidelity for storage and transfer of qubit states

which are encoded in the $|0\rangle$ and $|1\rangle$ Fock states of a harmonic oscillator, subjected to a Gaussian process. Since coherent states form a complete basis for the harmonic oscillator, the parameters characterizing a Gaussian process can be determined by its action on coherent states, and subsequently the action of the process on any class of quantum states can be obtained. The main result of our calculation is the explicit expression, Eq. (20), for the average qubit fidelity for a general Gaussian process. This expression shows how imperfect gain and added noise both contribute to the infidelity of protocols handling qubits in oscillator degrees of freedom. It also shows, however, that part of the infidelity may be recovered by merely redefining the phases of the qubit basis states.

There has already been considerable efforts to determine the fidelity of Gaussian operations acting on oscillators prepared in coherent states, squeezed states and qubit states, and in connection with the beam-splitter like coupling of light modes and atomic ensembles, the average qubit fidelity has been calculated in Ref. [8]. Our theory, indeed, reproduces that result when we restrict to symmetric gain and noise. Currently, however, there is a growing experimental interest in hybrid quantum system architectures, where, e.g., effective two-level systems are used for preparation and processing of qubit states, while oscillator systems are used for storage and transport. These systems apply different coupling schemes and frequently the couplings to the quadratures of the electromagnetic, mechanical or collective spin oscillators differ, leading to asymmetries in the (\hat{X}, \hat{P}) phase-space. Another source of asymmetry may occur during processing of the individual oscillator modes, as exemplified by π pulses applied to spin ensembles in Ref. [45]. The general expression Eq. (20) and the examples given in Sec. IV properly describe the fidelity of qubit manipulation in such hybrid systems.

ACKNOWLEDGMENTS

The authors acknowledge support from the EU Seventh Framework Programme collaborative project iQIT and the Villum Foundation.

-
- [1] D. P. DiVincenzo, *Science* **270**, 255 (1995).
 - [2] A. D. Boozer, A. Boca, R. Miller, T. E. Northup, and H. J. Kimble, *Phys. Rev. Lett.* **98**, 193601 (2007).
 - [3] H. P. Specht, C. Nölleke, A. Reiserer, M. Uphoff, E. Figueroa, S. Ritter, and G. Rempe, *Nature* **473**, 190 (2011).
 - [4] M. Riebe, H. Häffner, C. F. Roos, W. Hänsel, J. Benhelm, G. P. T. Lancaster, T. W. Körber, C. Becher, F. Schmidt-Kaler, D. F. V. James, and R. Blatt, *Nature* **429**, 734 (2004).
 - [5] M. D. Barrett, J. Chiaverini, T. Schaetz, J. Britton, W. M. Itano, J. D. Jost, E. Knill, C. Langer, D. Leibfried, R. Ozeri, and D. J. Wineland, *Nature* **429**, 737 (2004).
 - [6] S. L. Braunstein and P. van Loock, *Rev. Mod. Phys.* **77**, 513 (2005).
 - [7] A. Furusawa, J. L. Sørensen, S. L. Braunstein, C. A. Fuchs, H. J. Kimble, and E. S. Polzik, *Science* **282**, 706 (1998).
 - [8] J. F. Sherson, H. Krauter, R. K. Olsson, B. Julsgaard, K. Hammerer, I. Cirac, and E. S. Polzik, *Nature* **443**, 557 (2006).
 - [9] H. Krauter, D. Salart, C. A. Muschik, J. M. Petersen, H. Shen, T. Fernholz, and E. S. Polzik, *Nature Phys.* **9**, 400 (2013).

- [10] B. Julsgaard, J. Sherson, J. I. Cirac, J. Fiuràšek, and E. S. Polzik, *Nature* **432**, 482 (2004).
- [11] K. Honda, D. Akamatsu, M. Arikawa, Y. Yokoi, K. Akiba, S. Nagatsuka, T. Tanimura, A. Furusawa, and M. Kozuma, *Phys. Rev. Lett.* **100**, 093601 (2008).
- [12] J. Appel, E. Figueroa, D. Korystov, M. Lobino, and A. I. Lvovsky, *Phys. Rev. Lett.* **100**, 093602 (2008).
- [13] H. de Riedmatten, M. Afzelius, M. U. Staudt, C. Simon, and N. Gisin, *Nature* **456**, 773 (2008).
- [14] M. P. Hedges, J. J. Longdell, Y. Li, and M. J. Sellars, *Nature* **465**, 1052 (2010).
- [15] K. Hammerer, A. S. Sørensen, and E. S. Polzik, *Rev. Mod. Phys.* **82**, 1041 (2010).
- [16] W. Tittel, M. Afzelius, T. Chanelière, R. L. Cone, S. Kröll, S. A. Moiseev, and M. Sellars, *Laser & Photon. Rev.* **4**, 244 (2010).
- [17] D. Kleckner and D. Bouwmeester, *Nature* **444**, 75 (2006).
- [18] J. D. Thompson, B. M. Zwickl, A. M. Jayich, F. Marquardt, S. M. Girvin, and J. G. E. Harris, *Nature* **452**, 72 (2008).
- [19] T. J. Kippenberg, H. Rokhsari, T. Carmon, A. Scherer, and K. J. Vahala, *Phys. Rev. Lett.* **95**, 033901 (2005).
- [20] C. A. Regal, J. D. Teufel, and K. W. Lehnert, *Nature Phys.* **4**, 555 (2008).
- [21] D. Hunger, S. Camerer, T. W. Hänsch, D. König, J. P. Kotthaus, J. Reichel, and P. Treutlein, *Phys. Rev. Lett.* **104**, 143002 (2010).
- [22] C. W. Chou, H. de Riedmatten, D. Felinto, S. V. Polyakov, S. J. van Enk, and H. J. Kimble, *Nature* **438**, 828 (2005).
- [23] T. Chanelière, D. N. Matsukevich, S. D. Jenkins, S. Lan, T. A. B. Kennedy, and A. Kuzmich, *Nature* **438**, 833 (2005).
- [24] M. D. Eisaman, A. André, F. Massou, M. Fleischhauer, A. S. Zibrov, and M. D. Lukin, *Nature* **438**, 837 (2005).
- [25] Y. Kubo, C. Grezes, A. Dewes, T. Umeda, J. Isoya, H. Sumiya, N. Morishita, H. Abe, S. Onoda, T. Ohshima, V. Jacques, A. Dréau, J.-F. Roch, I. Diniz, A. Auffeves, D. Vion, D. Esteve, and P. Bertet, *Phys. Rev. Lett.* **107**, 220501 (2011).
- [26] C. Clausen, F. Bussièrès, M. Afzelius, and N. Gisin, *Phys. Rev. Lett.* **108**, 190503 (2012).
- [27] M. Gündoğan, P. M. Ledingham, A. Almasi, M. Cristiani, and H. de Riedmatten, *Phys. Rev. Lett.* **108**, 190504 (2012).
- [28] Z.-L. Xiang, S. Ashhab, J. Q. You, and F. Nori, *Rev. Mod. Phys.* **85**, 623 (2013).
- [29] P. Rabl, D. DeMille, J. M. Doyle, M. D. Lukin, R. J. Schoelkopf, and P. Zoller, *Phys. Rev. Lett.* **97**, 033003 (2006).
- [30] D. Petrosyan, G. Bensky, G. Kurizki, I. Mazets, J. Majer, and J. Schmiedmayer, *Phys. Rev. A* **79**, 040304(R) (2009).
- [31] J. H. Wesenberg, A. Ardavan, G. A. D. Briggs, J. J. L. Morton, R. J. Schoelkopf, D. I. Schuster, and K. Mølmer, *Phys. Rev. Lett.* **103**, 070502 (2009).
- [32] D. Marcos, M. Wubs, J. M. Taylor, R. Aguado, M. D. Lukin, and A. S. Sørensen, *Phys. Rev. Lett.* **105**, 210501 (2010).
- [33] A. D. O'Connell, M. Hofheinz, M. Ansmann, R. C. Bialczak, M. Lenander, E. Lucero, M. Neeley, D. Sank, H. Wang, M. Weides, J. Wenner, J. M. Martinis, and A. N. Cleland, *Nature* **464**, 697 (2010).
- [34] O. Arcizet, V. Jacques, A. Siria, P. Poncharal, P. Vincent, and S. Seidelin, *Nature Phys.* **7**, 879 (2011).
- [35] J.-M. Pirkkalainen, S. U. Cho, J. Li, G. S. Paraoanu, P. J. Hakonen, and M. A. Sillanpää, *Nature* **494**, 211 (2013).
- [36] X.-B. Wang, Z.-W. Yu, J.-Z. Hu, A. Miranowicz, and F. Nori, *Phys. Rev. A* **88**, 022101 (2013).
- [37] B. Julsgaard, C. Grezes, P. Bertet, and K. Mølmer, *Phys. Rev. Lett.* **110**, 250503 (2013).
- [38] R. Simon, E. C. G. Sudarshan, and N. Mukunda, *Phys. Rev. A* **36**, 3868 (1987).
- [39] M. Lobino, D. Korystov, C. Kupchak, E. Figueroa, B. C. Sanders, and A. I. Lvovsky, *Science* **322**, 563 (2008).
- [40] M. S. Kim, F. A. M. de Oliveira, and P. L. Knight, *Phys. Rev. A* **40**, 2494 (1989).
- [41] J. J. Gong and P. K. Aravind, *Am. J. Phys.* **58**, 1003 (1990).
- [42] C. W. Gardiner and M. J. Collett, *Phys. Rev. A* **31**, 3761 (1985).
- [43] D. Bouwmeester, J.-W. Pan, H. Weinfurter, and A. Zeilinger, *J. Mod. Opt.* **47**, 279 (2000).
- [44] C. W. Gardiner and P. Zoller, *Quantum Noise*, 2nd ed. (Springer, Berlin, 2000).
- [45] B. Julsgaard and K. Mølmer, arXiv:1309.5517.